CHEMISTRY
AN ASIAN JOURNAL

DOI: 10.1002/asia.200800099

Improvement of Photoaffinity SPR Imaging Platform and Determination of the Binding Site of p62/SQSTM1 to p38 MAP Kinase

Akiko Saito,[a] Kayoko Kawai,[a, b] Hiroshi Takayama,[a, b] Tatsuhiko Sudo,[a] and Hiroyuki Osada*[a, b]

Dedicated to Professor Ryoji Noyori on the occasion of his 70th birthday

Abstract: p38 mitogen-activated protein kinase (MAPK) is a member of the serine/threonine kinases and is activated in response to stress stimuli, such as cytokines, ultraviolet irradiation, heat shock, and osmotic shock. We revealed in a previous report that p62/SQSTM1, known to participate in proteasomal or autophagosomal protein degradation and cytokine receptor signal transduction pathways, binds to p38 to regulate specifically. Herein, we describe the improvement of the photoaffinity-thiol linker of our SPR imaging platform, which enabled us to determine the binding site of p62 to p38. SPR imaging experiments using a new photoaffinity linker **2** to immobilize the peptides derived from p62 on gold substrate indicate that the domain comprising amino acids 164–190 of p62 binds to p38 directly. These SPR analysis data and empirical biologic data reveal that the binding site of p62 to p38 is the domain corresponding to 173–182.

Keywords: biosensors · gold · peptides · photoaffinity labeling · surface plasmon resonance

Introduction

p38 mitogen-activated protein kinase (MAPK) has been identified as an anti-inflammatory drug binding protein, a lipopolysaccharide-activated protein kinase, or a stress-responsive protein kinase.[1] p38 is implicated as a mediator to transmit intracellular signaling for cell survival, differentiation, and response to stress, including various cytokines. We have studied to elucidate the precise molecular mechanism by which p38 can exert various responses to different stimuli,[2–4] and we previously showed that p62/SQSTM1, known as a phosphotyrosine-independent ligand for the $p56^{lck}$-SH domain,[5] bound to regulate p38 in vitro.[6] It is also known that p62 plays important roles in proteasomal or autophagosomal protein degradation[7,8] and cytokine receptor signal transduction pathways.[9,10] Our further biological studies, such as co-immunoprecipitation assays using deletion mutants of p62, revealed two domains that play an essential role for the interaction with p38, however, it was not clear whether both domains interacted with p38 directly. We thought that the SPR imaging technique was suitable for the determination of the binding site between p38 and p62 by detecting the SPR signals that were produced by the interaction between p38 and peptides derived from p62.

We have recently developed a "photoaffinity" surface plasmon resonance (SPR) imaging platform to enable the immobilization of structurally diverse small molecules on solid supports in a "functional group-independent" manner.[11] However, the SPR signals generated by the interaction between p38 and p62 were not detected under previously reported conditions. Herein, we describe the improvement of the photoaffinity-thiol linker of our SPR imaging platform to enable us to investigate the binding site of p62 to p38, and this new linker enables us to determine the binding site.

[a] Dr. A. Saito, K. Kawai, H. Takayama, Dr. T. Sudo, Dr. H. Osada
Antibiotics Laboratory
Chemical Biology Department
Advanced Research Institute, RIKEN
2-1 Hirosawa, Wako, Saitama, 351-0198 (Japan)
Fax: (+81) 48-462-4669
E-mail: hisyo@riken.jp

[b] K. Kawai, H. Takayama, Dr. H. Osada
Graduate School of Science and Engineering
Saitama University
255 Shimo-okubo, Saitama, 338-8570 (Japan)

Results and Discussion

Improvement of the Photoaffinity-Thiol Linker for SPR Imaging

In recent years, the SPR imaging technique has been used to observe multiple interactions between non labeled biological molecules and surface-bound molecules such as DNA,[12,13] protein,[14,15] peptide,[16] and small molecules[17,18] with an array format. However, most immobilization methods on a chip need a specific functional group to mediate covalent attachment to the solid surface. In the case of peptides, a specific amino acid sequence or biotin group on the peptide terminus is necessary for immobilization. It is implied that the amino acid sequence that can be immobilized is limited, or the structure of the immobilized peptide differs from the original structure by modifications, such as biotinylation. There are easy methods to immobilize either the C- or N-terminus of peptides to the chip. However, there are few methods to immobilize, in uniform condition, both C- and N-termini of peptides onto the solid surface. The immobilization method requiring the specific terminus of the peptide is not usable when the terminal sequence is responsible for the recognition of the binding partner. Once the terminal was used for the immobilization, the interaction of the peptide with the binding partner can not be observed.

We have recently developed a "photoaffinity-linking" protocol to enable the introduction of structurally diverse small molecules on solid supports in a "functional group-independent" manner.[19,20] In this protocol, small molecules are immobilized on a chip by a highly reactive carbene species generated from surface-bound aryl diazirine upon UV irradiation.[21–23] We confirmed that immobilized peptides on glass slides by our photoaffinity method were detectable with proteins known to bind to the peptide, and those results demonstrated the functional-group independency of the photoaffinity-linking method.[24] As mentioned above, we also reported the development of the photoaffinity SPR imaging platform to observe the interaction between nonlabeled proteins and nonmodified small-molecules on chips.[11] Thus, we thought that our SPR imaging technique was suitable for determination of the binding site between p38 and p62 using the detection of SPR signals produced by the binding of p38 to synthetic peptides derived from p62.

First, we used photoaffinity-thiol linker **1** (Figure 1), terminated with a phenyl-diazirine group, and dummy linker **5**, terminated with a hydroxyl group, reported previously,[11] to photochemically immobilize the p38-binding peptide MNSRKPDLRVVIPPSS derived from myocyte enhancer factor 2A (MEF2A), which is a specific substrate of p38, as a positive control, and its mutants MNS**AA**PDLRVVIPPSS and MNSRKPD**A**R**A**VIPPSS as negative controls.[25] However, in this model system, the SPR signals produced by the binding of p38 were too low to make a sharp contrast between the positive and negative signals (Figure 3b-A).

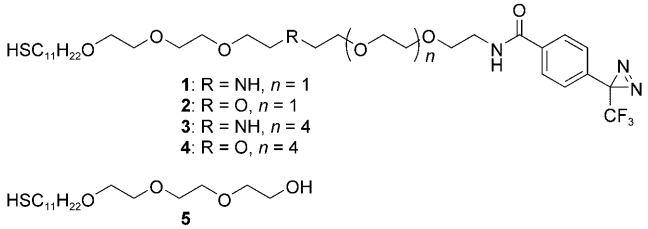

Figure 1. Structure of the photoaffinity linkers 1–4 and dummy linker **5**.

In the studies previously conducted, the SPR signals were often undetectable, although the interactions should theoretically be observed according to their dissociation constant. Hence, we decided to synthesize new linkers to re-examine the length of the polyethylene glycol (PEG) chain and the necessity of the NH group in the PEG chain.

We synthesized new photoaffinity-thiol linkers **2–4** (Figure 1), as shown in Scheme 1. Tri(ethyleneglycol) derivative **6** was oxidized with Dess–Martin Periodinane to an aldehyde and then coupled with aryl-diazirine derivative **8** by reductive amination to give **9** with a 22% yield from **6**. The deprotection of **9** afforded photoaffinity-thiol linker **3** in a 96% yield. Amino-thiols **10** and **11** were condensed with **12** to give **2** and **4** in 61% and 44% yields, respectively.

To evaluate the newly synthesized linkers, we prepared photoaffinity-linker-coated gold substrates (PGSs) from **1–4** to immobilize 11 digoxin analogs on gold surface, and these PGSs were treated with a mouse monoclonal anti-digoxin antibody (Figure 2). In our previous report, it was confirmed that the interaction between digoxin and its antibody was observed on a PGS coated with **1**.[11] In a structure–activity relationship (SAR) experiment with the photoaffinity small molecule microarray that we reported previously, the signal strength produced by the interaction of the digoxin analog and anti-digoxin antibody on the array significantly correlated with the results of the solution-phase binding assay.[24] So, the digoxin analog–digoxin antibody model system was thought to be appropriate for evaluation, whether the observed SPR signals on the PGSs coated with new photoaffinity linkers were reasonable or not. As shown in Figure 2, the observed SPR signals produced by the interaction of digoxin analogs and the anti-digoxin antibody were relatively

Abstract in Japanese:

細胞内シグナル伝達分子の一つである p38 MAP キナーゼは、刺激に反応して活性化されるセリン/スレオニンキナーゼである。我々は、p38 と p38 結合分子として同定された p62 (SQSTM1)との相互作用部位を特定するため、光親和型 SPR イメージング法を改良し、結合部位の同定に成功した。まず、我々は SPR イメージング法の感度を向上させるため、金基板に導入するチオールリンカーの改良を行い、GST-p38 と p38 に結合する事が知られているペプチドとの相互作用を高感度に検出できる系を開発した。次に、これまでの研究において p38 と相互作用すると予想された p62 の配列に対応するペプチドを合成して金基板上に固定化し、GST-p38 との相互作用による SPR シグナルの検出を試みた。その結果、GST-p38 は、p62 の 164-190 番目に対応するペプチドに直接結合し、特に 178-190 番目に対応するペプチド GFSHSRWLRKVKH に最も強く結合する事が確認された。

CHEMISTRY
AN ASIAN JOURNAL

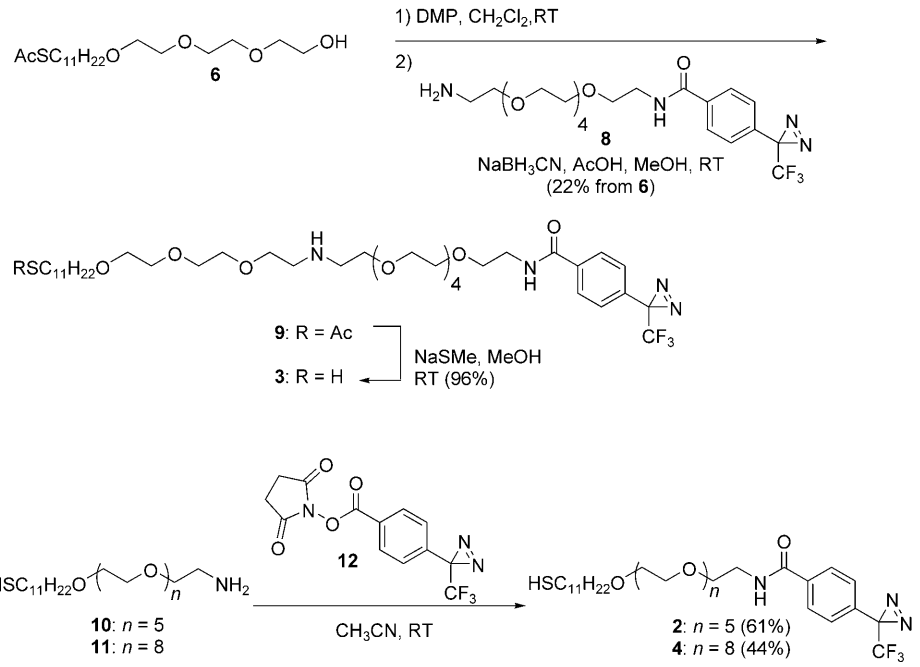

Scheme 1. Synthesis of the photoaffinity-thiol linkers.

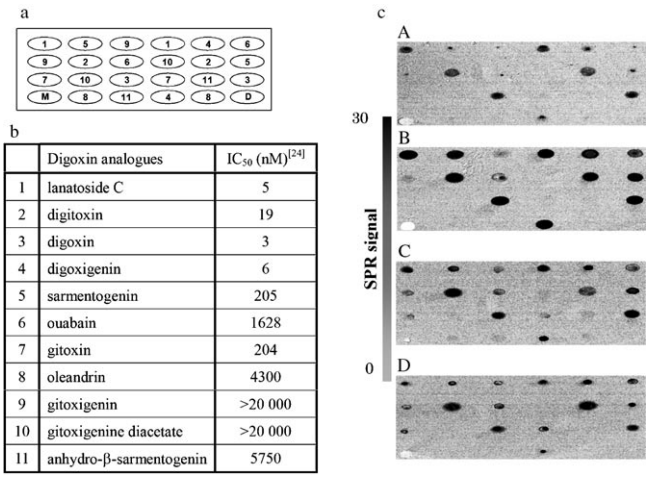

	Digoxin analogues	IC_{50} (nM)[24]
1	lanatoside C	5
2	digitoxin	19
3	digoxin	3
4	digoxigenin	6
5	sarmentogenin	205
6	ouabain	1628
7	gitoxin	204
8	oleandrin	4300
9	gitoxigenin	>20 000
10	gitoxigenine diacetate	>20 000
11	anhydro-β-sarmentogenin	5750

Figure 2. Comparison and evaluation of new photoaffinity-thiol linkers. Interaction between digoxin analogs and anti-digoxin antibody on PGS coated with photoaffinity-thiol linker **1**–**4**. a) The array pattern of the immobilized digoxin analogs. M: marker to fit spot area for SPR signal analysis; D: DMSO. b) Immobilized digoxin analogs and their IC_{50}, value, which was determined by the solution-phase binding assay.[24] c) Observed SPR difference images when the gold substrate coated with each photoaffinity linker (**1**–**4**) was treated with a solution of anti-digoxin antibody (8 μg mL^{-1}); A) **1** (0.1 mM) and **5** (0.9 mM), B) **2** (0.1 mM) and **5** (0.9 mM), C) **3** (0.1 mM) and **5** (0.9 mM), D) **4** (0.1 mM) and **5** (0.9 mM).

reasonable in all cases, and the new linkers improved detection sensitivity. In particular, the PGS that was coated with linker **2** gave sufficient results for analysis of the interaction of digoxin analogs and anti-digoxin antibody in terms of good S/N ratio, sensitivity, and shape of the spots (Figure 2c-B).[26] As shown in Figure 2c-A, C, and D, the spot size differed with each compound, although the signal strength was enough to evaluate the interaction between digoxin analogues and anti-digoxin antibody. These spots had a high tendency to vary in size on the PGSs coated with **1** and **3**, being the NH-group including linkers. However, we have not reached a conclusion about the optimal structure of the photoaffinity linker for this platform, because this tendency of a shrinking in the size of the spots was also observed with linker **4**.

Proof-of-Concept Study and Determination of the Binding Site Between p38 and p62[27]

Next, we used new linkers **2**–**4** in the foregoing "p38-MEF2A" model system in a proof-of-concept study (Figure 3B–D). The best result was again obtained with linker **2**. The SPR signals produced by p38 binding to peptides on a PGS coated with **2**, were enough to estimate the differences between positive control and negative controls, and gave good S/N ratios. The nonspecific background signals tended to be high on PGSs coated with NH-group including linkers. Although the increasing SPR signals of the experiments with linkers **3** and **4** were low, they tended to be similar to the signal obtained with linker **2**. These results indicated that this SPR imaging system worked well to detect specific binding to p38.

Since the proof-of-concept study was successful, the practical application of the SPR imaging technique to determine the binding site between p62 and p38 was performed (Figure 4). Further to MEF2A-related peptides, six peptides derived from p62, thought to play important roles in binding to p38 in previous biological assays,[27] were arrayed on a chip that was coated with linker **2** (Figure 4a). The SPR imaging study indicated that the three peptides 6, 9, and 10, corresponding to amino acids 164–190 of p62, bound to p38 directly, and peptide 10, corresponding to 178–190, bound to p38 the strongest.[28] These results are in reasonable agreement with the empirical biologic results, suggesting that the domain comprising amino acids 173–182 of p62 is essential for binding to p38. However, it was indicated that the domain corresponding to 330–342, peptide 5, was also very important for binding in the biological assay; this SPR imaging experiment revealed that the direct interaction between p38 and peptide 5 was smaller as compared with the interaction of p38 to peptides 6, 9, and 10. So, we speculate that p38 can bind to the domain comprising amino acids 164–190 of p62 directly, and that, another important domain compris-

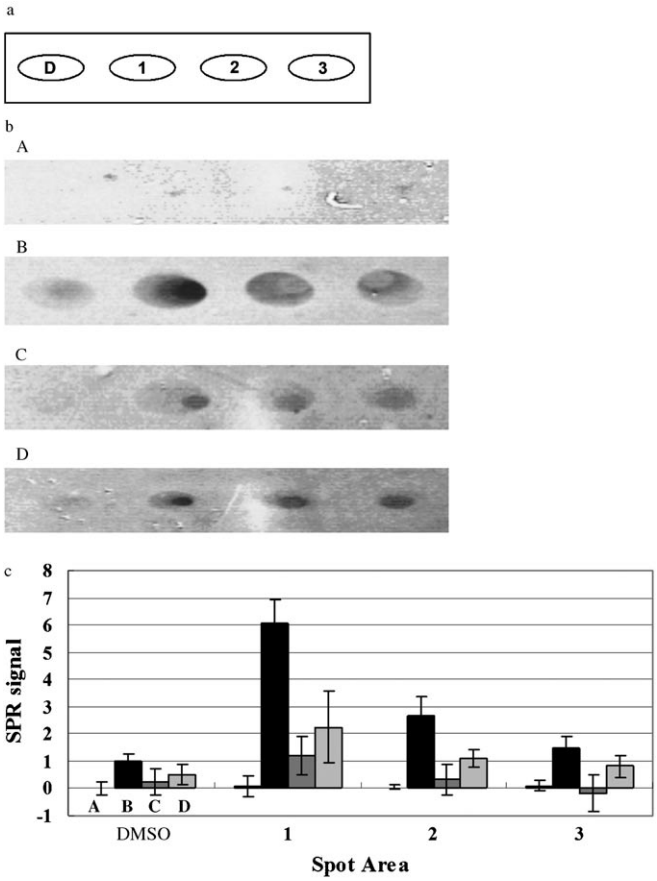

Figure 3. Proof-of-concept study: Detection of the interaction between p38 and control peptides derived from MEF2A. SPR difference images showing the binding of GST-p38 to control peptides examined on PGSs. a) DMSO solution of peptides (10 mM) was spotted to the areas designated below: D: DMSO; 1: MNSRKPDLRVVIPPSS (positive control); 2: MNSAAPDLRVVIPPSS (negative control); 3: MNSRKPDARAVIPPSS (negative control). b) Observed SPR difference images when the gold substrate coated with each photoaffinity-thiol linker (**1**–**4**) was treated with a solution of GST-p38 (0.3 mg mL^{-1}); A) **1** (0.1 mM) and **5** (0.9 mM), B) **2** (0.1 mM) and **5** (0.9 mM), C) **3** (0.1 mM) and **5** (0.9 mM), D) **4** (0.1 mM) and **5** (0.9 mM). c) Increase of SPR signal by incubation with GST-p38 for 10 min. **A**–**D** correspond to A)–D) of (b). Each entry represents the average of six spots.

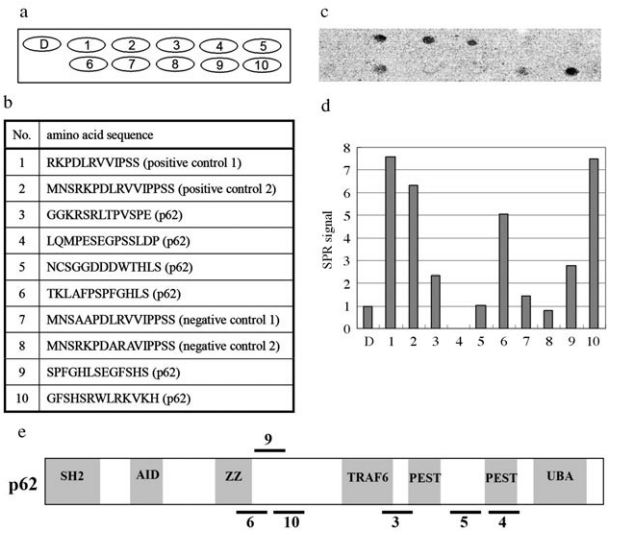

No.	amino acid sequence
1	RKPDLRVVIPSS (positive control 1)
2	MNSRKPDLRVVIPPSS (positive control 2)
3	GGKRSRLTPVSPE (p62)
4	LQMPESEGPSSLDP (p62)
5	NCSGGDDDWTHLS (p62)
6	TKLAFPSPFGHLS (p62)
7	MNSAAPDLRVVIPPSS (negative control 1)
8	MNSRKPDARAVIPPSS (negative control 2)
9	SPFGHLSEGFSHS (p62)
10	GFSHSRWLRKVKH (p62)

Figure 4. Determination of the binding site of p62 to p38. Detection of the interaction between peptides derived from p62 and GST-p38. a) Array design of the immobilized peptides. 1–10 show the spot area of each peptide. b) The amino acid sequence of the synthesized peptide. c) Observed SPR difference image when the gold substrate coated with photoaffinity-thiol linker **2** and dummy linker **5** was treated with a solution of GST-p38 (0.3 mg mL^{-1}). d) Increase of SPR signal by incubation with GST-p38 for 10 min normalized by the signal strength of DMSO. Each entry represents the average of two spots. e) The association domain of p62 to p38 identified in this SPR imaging experiment. Black bars and numbers show the approximate regions of synthetic peptides in p62. SH2, AID, ZZ, TRAF6, PEST, and UBA indicate the domains that interact with the respective binding proteins or participate in the stability of proteins.

ing amino acids 330–342 has another role in the interaction between p38 and p62, such as a role to form a certain conformation suitable for association with p38. Furthermore, peptide 3, which includes cationic amino acid residues, bound weakly to p38, and peptide 4—which includes the PESE sequence with homology to PXSP, the substrate sequence of p38—did not bind to p38.

Conclusions

Our photoaffinity SPR imaging platform is significantly improved by reviewing the thiol linkers used to coat the surface of the gold substrate. New photoaffinity linkers **2** and **3** allow the identification of the binding site between p38 and p62. Notably, linker **2** improves the signal strength and S/N ratio of SPR signals of the protein–peptide interaction, which was difficult to analyze by SPR imaging experiments using conventional linker **1**. Furthermore, the new linkers also improve the detection sensitivity of the interactions between not only peptides and proteins but also small molecules and proteins. We have confirmed some cases that the linker **3** is suitable in SPR experiments using different proteins and other series of small molecules, although linker **2** gave good results for the binding site determination of p38 and p62. Unfortunately, we are yet to find a generally applicable linker. Therefore, further studies on the improvement of this SPR platform and screening of new bioprobes are in progress.

Experimental Section

Synthesis

All commercially available chemicals for chemical synthesis were used without further purification. All reactions were carried out under an argon atmosphere and monitored by thin-layer chromatography with 0.25 mm pre-coated silica gel plates 60F254 Art 5715 (Merck, Darmstadt, Germany) and FUJI SILYSIA CHEMICAL LDT Chromatorex 0.25 mm NH-silica gel plates (Fuji Silysia Chemical LDT, Aichi, Japan). For silica-gel column chromatography, Silica gel 60 N (Kanto Chemical Co., Inc., Tokyo, Japan) and NH-silica gel (Fuji Silysia Chemical LDT, Aichi, Japan) were utilized. ^{1}H NMR spectra were recorded on a JEOL JNM-

AL400 spectrometer. Fast atom bombardment (FAB) mass spectra were obtained using a JMS-HX110 mass spectrometer.

Photoaffinity-thiol linker 3: Dess–Martin Periodinane (182 mg, 0.43 mmol) was added to a solution of **6**[29] (81.0 mg, 0.21 mmol) in CH_2Cl_2 (10 mL) at room temperature (RT). After the reaction mixture had been stirred for 6 h, it was filtered through a celite pad and concentrated in vacuo. AcOH (13 μL, 0.22 mmol) and $NaBH_3CN$ (7.8 mg, 0.12 mmol) were added to a solution of the crude aldehyde (100 mg) and amine **8**[24] (50.0 mg, 0.11 mmol) in methanol at RT and stirred for 12 h at this temperature. The reaction was quenched with saturated aqueous solution of $NaHCO_3$ (5 mL), and concentrated in vacuo. The residue was diluted with water (5 mL) and extracted with EtOAc (10 mL×3). The organic layers were washed with brine (5 mL), dried over Na_2SO_4, filtered, and concentrated in vacuo. The residue was purified by NH-silica gel column chromatography ($CHCl_3$/MeOH=15:1) to afford **9** (20 mg, 0.023 mmol, 22%) as a pale yellow oil.

An aqueous solution of NaSMe (0.17 mL, 15%, 0.35 mmol) was added to a solution of **9** (20.0 mg, 0.023 mmol) in MeOH (3 mL) at RT. The reaction mixture was stirred for 2 h at RT, then quenched with water (3 mL), and concentrated in vacuo. The residue was diluted with water (5 mL) and extracted with EtOAc (10 mL×3). The organic layers were washed with brine (5 mL), dried over Na_2SO_4, filtered, and concentrated in vacuo. The residue was purified by NH-silica gel column chromatography ($CHCl_3$/MeOH=15:1) to give thiol linker **3** (18 mg, 0.022 mmol, 96%) as a pale yellow oil. **9**: ^{1}H NMR (400 MHz, $CDCl_3$): δ=7.84 (2H, d. J=8.4 Hz), 7.21 (2H, d, J=8.4 Hz), 7.04 (1H, br), 3.64–3.48 (32H, m), 3.40 (2H, t, J=6.8 Hz), 2.76 (2H, dt, J=3.1, 5.3 Hz), 2.65 (2H, t, J=7.2 Hz), 2.10–1.99 (2H, br), 1.64 (2H, dt, J=7.0, 14.8 Hz), 1.53 (2H, dt, J=7.0, 14.0 Hz), 1.40–1.20 ppm (16H, m); FAB-MS m/z (%): 55 (100), 782 (6.3), 784 (8.3), 810 (5.0), 811 (5.2) $[M+H]^+$; HR-FAB-MS (NBA) m/z (%) calcd for $C_{38}H_{66}F_3N_4O_9S$: 811.4503 $[M+H]^+$; found 811.4519.

Photoaffinity-thiol linker 2: **12**[30] (22.5 mg, 0.068 mmol) was added to a solution of **10**[31] (44.0 mg, 0.086 mmol) in CH_2Cl_2 (10 mL) at RT. After the reaction mixture had been stirred for 2 h, it was concentrated in vacuo. The residue was purified by silica-gel column chromatography ($CHCl_3$/MeOH=10:1) to give thiol linker **2** (39.0 mg, 0.057 mmol, 61%) as a pale yellow oil. **2**: ^{1}H NMR (400 MHz, $CDCl_3$): δ=7.83 (2H, d, J=7.9 Hz), 7.23 (2H, d, J=7.9 Hz), 6.92 (1H, br), 3.65–3.52 (22H, m), 3.41 (2H, t, J=6.7 Hz), 2.65 (2H, t, J=7.1 Hz), 1.93–1.91 (1H, br), 1.81–1.61 (2H, m), 1.56–1.52 (2H, m), 1.35–1.18 ppm (16H, m); FAB-MS m/z (%): 55 (52), 185 (60), 228 (100), 229 (41), 256 (52), 650 (5.5), 652 (4.4), 678 (16) $[M+H]^+$-2H 679 (7.1), 680 (3.7); HR-FAB-MS (NBA) m/z (%) calcd for $C_{32}H_{51}F_3N_3O_7S$: 678.3400 $[M+H]^+$-2H; found 678.3419.

Photoaffinity-thiol linker 4: **12** (32.0 mg, 0.10 mmol) was added to a solution of **11** (30.0 mg, 0.050 mmol) in CH_2Cl_2 (10 mL) at RT. After the reaction mixture had been stirred for 12 h, it was concentrated in vacuo. The residue was purified by silica gel column chromatography ($CHCl_3$/MeOH=10:1) to give thiol linker **4** (18.0 mg, 0.022 mmol, 44%) as a pale yellow oil. **4**: ^{1}H NMR (400 MHz, $CDCl_3$): δ=7.83 (2H, d, J=8.5 Hz), 7.21 (2H, d, J=8.5 Hz), 6.94 (1H, brs), 3.66–3.53 (34H, m), 3.41 (2H, t, J=6.8 Hz), 2.65 (2H, t, J=7.2 Hz), 2.18–2.01 (1H, br), 1.64 (2H, m), 1.52 (2H, m), 1.35–1.24 ppm (16H, m); FAB-MS m/z (%): 55 (75), 73 (100), 228 (75), 404 (38), 417 (34), 502 (15), 810 (7.3) $[M+H]^+$-2H, 811 (3.2); HR-FAB-MS (NBA) m/z (%) calcd for $C_{38}H_{63}F_3N_3O_{10}S$: 810.4186 $[M+H]^+$-2H; found 810.4204.

Peptides: Peptides were synthesized by Research Resources Center/Brain Science Institute/RIKEN. We designed the peptides as follows. RKPDLRVVIPSS (positive control: corresponding to amino acids 269–281 of MEF2A); MNSRKPDLRVVIPPSS (positive control: corresponding to 266–281 of MEF2A); MNSAAPDLRVVIPPSS (negative control: MEF2A mutant 1); MNSRKPDARAVIPPSS (negative control: MEF2A mutant 2); GGKRSRLTPVSPE (corresponding to 262–274 of p62); LQMPESEGPSSLDP (corresponding to 356–369 of p62); NCSGGDDDWTHLS (corresponding to 330–342 of p62); TKLAFPSPFGHLS (corresponding to 164–176 of p62); SPFGHLSEGFSHS (corresponding to 170–182 of p62); GFSHSRWLRKVKH (corresponding to 178–190 of p62).

Preparation of the Recombinant Protein

The GST-hp38 expression plasmid was expressed in a bacterial strain, BL21 (DE3), and grown in LB media (100 μg mL^{-1} ampicillin) at 37°C until the cell density reached an A_{600} of 0.8. The culture was induced with IPTG (1 mM) and incubated at 37°C for 2 h. The harvested bacterial cells were resuspended in lysis buffer (50 mM Tris, pH 7.5, 25% sucrose) with lysozyme (0.2 mg mL^{-1}) and $MgCl_2$ (0.01 mM). On ice for 1 h, flash-frozen cells were thawed twice, and lysed by adding Nonidet P-40 (1%) followed by gentle sonication. After centrifugation at 10000 rpm for 15 min at 4°C, the supernatant was mixed with glutathione-agarose beads (SIGMA, 1 mL, 50%) and rotated at 4°C. After 2 h, the beads were poured into a column and washed with wash buffer (20 mL, 20 mM Tris, pH 7.5, 2 mM $MgCl_2$, 1 mM DTT). Fusion protein was eluted with elution buffer (5 mM GSH, 50 mM Tris, pH 9.6) and dialyzed into PBS with glycerol (10%).

Preparation of Photoaffinity-Linker-Coated Gold Substrates (PGSs) or Digoxin Analogs and Peptide Printing on PGSs

The PGSs were prepared according to our previous report[11] with each synthesized new photoaffinity linker. A gold-coated glass chip (TOYOBO, Japan) was immersed in the ethanol solution, which contained photoaffinity linker (0.1 mM of each) and dummy linker **5** (0.9 mM), for 12 h. The chip was rinsed successively with ethanol, water, and ethanol, and dried to obtain a photo-reactive chip. DMSO solutions of digoxin analogs (10 mM) or peptides were applied onto the chip by using a MultiSprinter automated spotter (TOYOBO, Japan). The obtained chip was dried in vacuo, and then irradiated at 365 nm under a UV transmission filter (Sigma-Koki, Japan) with a CL-1000 L ultraviolet cross-linker (UVP Inc. CA, USA). The irradiation energy on the chip amounted to 2.8 J cm^{-2}.[32] The chip was washed with DMSO for 6 h, and then rinsed with water and ethanol.

Detection of Digoxin Analogs-Anti-Digoxin Antibody Interaction on PGS

The digoxin analog-immobilized gold substrate was placed into MultiSprinter SPR imaging instruments (TOYOBO, Japan) and incubated with BSA (0.1%) in running buffer (10 mM HEPES, 150 mM NaCl, pH 7.4) for 5 min. After washing with running buffer, a solution of mouse monoclonal anti-digoxin antibody clone DI-22 (Sigma–Aldrich Inc., MO, USA) (0.1 mL, 8 μg mL^{-1}) in running buffer was injected to the array surface at 0.1 mL min^{-1} and incubated for 10 min. All SPR experiments were performed at 30°C. The SPR image and signal data were collected with an SPR analysis program (TOYOBO, Japan). The SPR difference image was constructed by using a Scion Image (Scion, MD) program.

Detection of p38-Peptide Interaction on PGS

The peptide-immobilized gold substrate was placed into SPR imaging instruments (TOYOBO, Japan), and incubated with BSA (0.1%) in running buffer (10 mM Hepes, 150 mM NaCl, pH 7.4) for 5 min. After washing with running buffer, a solution of GST-hp38 (0.1 mL, 0.3 mg mL^{-1}) in running buffer was injected to the array surface at 0.1 mL min^{-1} and incubated for 10 min. All SPR experiments were performed at 30°C. The SPR image and signal data were collected with an SPR analysis program (TOYOBO, Japan). The SPR difference image was constructed by using a Scion Image (Scion, MD) program.

Acknowledgements

We thank Dr. Naoki Kanoh (Tohoku University) for insightful discussion. This work was supported in part by the Grant-in-Aid for Creative Scientific Research from the Ministry of Education, Culture, Sports, Science, and Technology of Japan to H.O. (No. 17GS0221).

[1] M. Raman, W. Chen, M. H. Cobb, *Oncogene* **2007**, *26*, 3100–3112.
[2] M. Matsumoto, T. Sudo, T. Saito, H. Osada, M. Tsujimoto, *J. Biol. Chem.* **2000**, *275*, 31155–31161.

[3] Y. Yagasaki, T. Sudo, H. Osada, *FEBS Lett.* **2004**, *575*,136–140.
[4] T. Sudo, K. Kawai, H. Matsuzaki, H. Osada, *Biochem. Biophys. Res. Commun.* **2005**, *337*, 415–421.
[5] I. Park, J. Chung, C. T. Walsh, Y. Yun, J. L. Strominger, J. Shin, *Proc. Natl. Acad. Sci. USA* **1995**, *92*, 12338–12342.
[6] T. Sudo, M. Maruyama, H. Osada, *Biochem. Biophys. Res. Commun.* **2000**, *269*, 521–525.
[7] G. Bjorkoy, T. Lamark, A. Brech, H. Outzen, M. Perander, A. Overvatn, H. Stenmark, T. Johansen, *J. Cell Biol.* **2005**, *171*, 603–614.
[8] M. L. Seibenhener, J. R. Babu, T. Geetha, H. Wong, N. R. Krishna, M. W. Wooten, *Mol. Cell. Biol.* **2004**, *24*, 8055–8068.
[9] A. Duran, M. Serrano, M. Leitges, J. M. Flores, S. Picard, J. P. Brown, J. Moscat, M. T. Diaz-Meco, *Dev. Cell* **2004**, *6*, 303–309.
[10] J. Moscat, M. T. Diaz-Meco, A. Albert, S. Campuzano, *Mol. Cell* **2006**, *23*, 631–640.
[11] N. Kanoh, M. Kyo, K. Inamori, A. Ando, A. Asami, A. Nakao, H. Osada, *Anal. Chem.* **2006**, *78*, 2226–2230.
[12] E. A. Smith, M. Kyo, H. Kumasawa, K. Nakatani, I. Saito, R. M. Corn, *J. Am. Chem. Soc.* **2002**, *124*, 6810–6811.
[13] M. Kyo, T. Yamamoto, H. Motohashi, T. Kamiya, T. Kuroita, T. Tanaka, J. D. Engel, B. Kawakami, M. Yamamoto, *Genes Cells* **2004**, *9*, 153–164.
[14] M. Piliarik, H. Vaisocherova, J. Homola, *Biosens. Bioelectron.* **2005**, *20*, 2104–2110.
[15] H. J. Lee, Y. Yan, G. Marriott, R. M. Corn, *J. Physiol.* **2004**, *563*, 61–71.
[16] K. Inamori, M. Kyo, Y. Nishiya, Y. Inoue, T. Sonoda, E. Kinoshita, T. Koike, Y. Katayama, *Anal. Chem.* **2005**, *77*, 3979–3985.
[17] D. J. Vetter, *J. Cell. Biochem.* **2002**, *87*, 79–84.
[18] J. M. McDonnell, *Curr. Opin. Chem. Biol.* **2001**, *5*, 572–577.
[19] N. Kanoh, S. Kumashiro, S. Simizu, Y. Kondoh, S. Hatakeyama, H. Tashiro, H. Osada, *Angew. Chem.* **2003**, *115*, 5742–5745; *Angew. Chem. Int. Ed.* **2003**, *42*, 5584–5587.
[20] N. Kanoh, T. Nakamura, K. Honda, H. Yamakoshi, Y. Iwabuchi, H. Osada, *Tetrahedron*, in press.
[21] J. Brunner, H. Senn, F. M. Richards, *J. Biol. Chem.* **1980**, *255*, 3313–3318.
[22] I. Caelen, H. Gao, H. Sigrist, *Langmuir* **2002**, *18*, 2463–2467.
[23] J. C. Miller, H. Zhou, J. Kwekel, R. Cavallo, J. Burke, E. B. Butler, B. S. Teh, B. B. Haab, *Proteomics* **2003**, *3*, 56–63.
[24] N. Kanoh, A. Asami, M. Kawatani, K. Honda, S. Kumashiro, H. Takayama, Si. Simizu, T. Amemiya, Yasumitsu Kondoh, S. Hatakeyama, K. Tsuganezawa, R. Utata, A. Tanaka, S. Yokoyama, H. Tashiro, H. Osada, *Chem. Asian J.* **2006**, *1*, 789–797.
[25] S. H. Yang, A. Galanis, A. D. Sharrocks, *Mol. Cell. Biol.* **1999**, *19*, 4028–4038.
[26] We also synthesized other various photoaffinity-thiol linkers and used them for the SPR imaging studies. However, the SPR signals produced by the interaction of small molecules and proteins were very low or not reasonable.
[27] We have already published the report focused on biological experiments. K. Kawai, A. Saito, T. Sudo, H. Osada, *J. Biochem.*, **2008**, DOI: 10.1093/jp/mvn027.
[28] Similar results were provided in the experiment using linker **3** as immobilizing linker of peptides on a chip (data not shown).
[29] C. Pale-Grosdemange, E. S. Simon, K. L. Prime, G. M. Whitesides, *J. Am. Chem. Soc.* **1991**, *113*, 12–21.
[30] A. I. Meyers, D. L. Temple, D. Haidukewych, E. D. Mihelich, *J. Org. Chem.* **1974**, *39*, 2787–2793.
[31] Q. Yu, S. Chen, A. D. Taylor, J. Homola, B. Hock, S. Jiang, *Sens. Actuators B* **2005**, *107*, 193–201.
[32] The alkanetiolate SAM on the PGS was not destroyed by exposure to UV light at 365 nm. We confirmed the stability of SAM on the PGS by X-ray photoelectron spectroscopy (XPS) in previous report.[11]

Received: March 14, 2008
Published online: July 21, 2008

